ISSN 1560-3547, Regular and Chaotic Dynamics, 2010, Vol. 15, Nos. 2–3, pp. 348–353. © Pleiades Publishing, Ltd., 2010.

L.P. SHILNIKOV–75
Special Issue

Example of Blue Sky Catastrophe Accompanied by a Birth of Smale–Williams Attractor

S. P. Kuznetsov*

Kotel'nikov's Institute of Radio-Engineering and Electronics of RAS, Saratov Branch, Zelenaya str., 38, Saratov, 410019, Russia
and
Department of Physics and Astronomy, University of Potsdam, Karl-Liebknecht-Str. 24/25, D-14476 Potsdam-Golm, Germany

Received February 24, 2010; accepted March 3, 2010

Abstract—A model system is proposed, which manifests a blue sky catastrophe giving rise to a hyperbolic attractor of Smale–Williams type in accordance with theory of Shilnikov and Turaev. Some essential features of the transition are demonstrated in computations, including Bernoulli-type discrete-step evolution of the angular variable, inverse square root dependence of the first return time on the bifurcation parameter, certain type of dependence of Lyapunov exponents on control parameter for the differential equations and for the Poincaré map.

MSC2000 numbers: 34C28, 34C23, 37D20, 37E99, 37G15, 37G35

DOI: 10.1134/S1560354710020206

Key words: attractor, bifurcation, Smale–Williams solenoid, Lyapunov exponent

Uniformly hyperbolic strange attractors have strong chaotic properties and allow for far-reaching mathematical analysis [1–7]. They are structurally stable, i.e. insensitive in respect to variations of functions and parameters in the governing equations. Traditionally, in reviews and textbooks on nonlinear dynamics, the uniformly hyperbolic attractors are illustrated by artificially constructed discrete-time evolution rules (Plykin attractor, Smale–Williams solenoid). An interesting problem is search for examples of such attractors in systems of physical or technical origin [8, 9]. Certainly, one possible direction of thought is consideration of *scenarios* of appearance of the hyperbolic chaotic attractors in nonlinear dissipative systems under variation of their control parameters.[1)]

Possible occurrence of the hyperbolic strange attractors was discussed by Ruelle, Takens, and Newhouse in a framework of generic phenomena accompanying destruction of quasiperiodic motions on tori of dimension 3 and more [10, 11], but they did not present concrete examples. More recently, Shilnikov and Turaev [12, 13] indicated a possibility of appearance of attractors of Smale–Williams type in Poincaré section of continuous-time systems undergoing a kind of the so-called blue sky catastrophe.

In the simplest version, a blue sky catastrophe occurs in three-dimensional phase space. At the bifurcation, a saddle-node limit cycle takes place, from which the trajectories depart along the unstable manifold, and return back to the same cycle from the opposite side. With a shift of a value of the control parameter in one direction, the saddle-node cycle transforms to a pair of close limit cycles, one stable and another unstable. With a parameter shift in the opposite direction, the saddle-node cycle disappears; instead, an attracting large-scale limit cycle emerges containing helical coils near the former saddle-node cycle.

Having initial angular coordinate φ near the saddle-node cycle, after a travel along the unstable manifold and subsequent return, the angular coordinate is expressed by relation, which contains, in general, an additive term $m\varphi$; for the three-dimensional case, the integer m may be equal 0 or 1. However, at higher dimensions, any integer can occur. In particular, $m = 2$ corresponds to a birth

*E-mail: spkuz@rambler.ru

[1)]This matter certainly is different from the commonly known scenarios of transition to chaos (like Feigenbaum's one), which lead to the onset of non-hyperbolic attractors.

of hyperbolic strange attractor represented by a Smale–Williams solenoid in Poincaré section. The authors [12, 13] stress that due to such bifurcation, a system of Morse – Smale class with simple dynamical behavior, immediately turns to a system with complex dynamics associated with the structurally stable chaotic attractor.

To my knowledge, no concrete systems with the last variant of the blue sky bifurcation were described in the literature. Known examples of the blue sky catastrophes relate to the three-dimensional case, when the hyperbolic chaotic attractor cannot arise [14–16].

To construct an example with birth of the Smale–Williams attractor, one must have the phase space dimension at least equal four. The phase-space flow has to be organized in such way that a toroidal domain close initially to the saddle-node cycle, in the course of travel and return back to that cycle would form a double-folded loop, with thinner coils. To do this, an idea advanced in our previous work with Pikovsky [17] may be applied with certain modifications.

Let us start with a two-dimensional predator – prey system with an instant state specified by two non-negative variables r_1, r_2:

$$\dot r_1 = 2(1 - r_2 + \tfrac{1}{2}r_1 - \tfrac{1}{50}r_1^2)r_1,\ \ \dot r_2 = 2(r_1 - \mu + \tfrac{1}{2}r_2 - \tfrac{1}{50}r_2^2)r_2. \tag{1}$$

These equations differ from those in Ref. [17] with additional nonlinear terms in the second ("predator") equation, and contain a control parameter μ. If the value of μ is slightly less than $\mu_0 = 3\frac{1}{8}$, a picture of orbits on the phase plane r_1, r_2 looks like that shown in Fig. 1a. There are four fixed points here, an unstable focus A, saddles B and C_1, and a node C_2. With increase of μ, the fixed points C_1 and C_2 move to meet each other at $\mu = \mu_0$, and then disappear (see the panels (b) and (c), respectively). Instead of the former pair of fixed points, a domain of relatively slow motion appears there, while the attractor is a limit cycle, which passes close to the origin and to the saddle B.

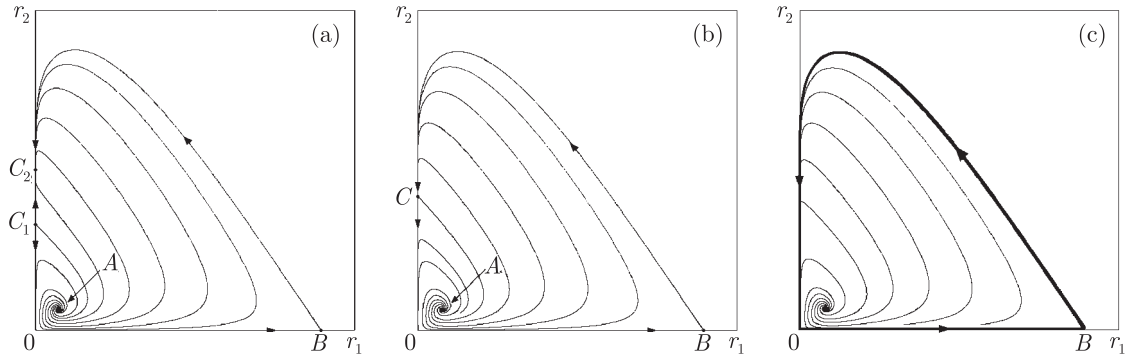

Fig. 1. Phase portraits of the system (1) with increase of μ from (a) to (c). Two fixed points, a stable node C_2 and a saddle C_1 (a) meet together at the bifurcation (b), and a limit cycle appears shown with a bold curve (c)

.

Following [17], let us consider the quantities r_1, r_2 as squared absolute values of complex amplitudes for two oscillators of some frequency ω_0, namely, $r_{1,2} = |a_{1,2}|^2$. One can write down a set of differential equations for the complex variables a_1, a_2, and add terms of certain form, which introduce additional coupling between the oscillators. The equations read

$$\begin{aligned}\dot a_1 &= -i\omega_0 a_1 + (1 - |a_2|^2 + \tfrac{1}{2}|a_1|^2 - \tfrac{1}{50}|a_1|^4)a_1 + \tfrac{1}{2}\varepsilon \mathrm{Im} a_2^2,\\ \dot a_2 &= -i\omega_0 a_2 + (|a_1|^2 - \mu + \tfrac{1}{2}|a_2|^2 - \tfrac{1}{50}|a_2|^4)a_2 + \varepsilon \mathrm{Re} a_1,\end{aligned} \tag{2}$$

where the added terms contain the coefficient ε. As a_1, a_2 are complex, in real dynamical variables (Rea_1, Ima_1, Rea_2, Ima_2) this is a four-dimensional system.

At $\varepsilon = 0$, equations for $r_{1,2} = |a_{1,2}|^2$ derived from (2) coincide precisely with Eqs. (1). At ε small enough, and at values of μ notably less than μ_0, the sustained dynamics presented graphically on

the plane r_1, r_2 is located close to the node C_2. For nonzero ε, this is a limit cycle of such kind that the second oscillator has some notable amplitude, while for the first one the amplitude is very small. Besides, there is a close unstable limit cycle close to C_1. With graduate increase of the parameter, both cycles come closer, meet together and coincide at some $\mu = \mu_c(\varepsilon) \approx \mu_0$, forming a semi-stable limit cycle. At $\mu > \mu_c(\varepsilon)$ it disappears. Now, motion of a representative point on the plane r_1, r_2 follows approximately a closed large-scale path, like in Fig. 1c, visiting again and again a neighborhood of the origin. Qualitatively, for each such passage, the following stages may be specified: excitation of the first oscillator (i), excitation of the second oscillator (ii), damping of the first oscillator (iii), and slower damping of the second oscillator (iv). Activation of the second oscillator occurs in presence of driving from the partner, due to the coupling term proportional to ε in the second equation, so, it inherits the phase from the first oscillator. During the damping stage of the second oscillator, its residual oscillations initiate activation of the first one. The corresponding term proportional to ε in the first equation contains squared complex amplitude, so, this transfer of excitation is accompanied with doubling of the argument of the complex variable, representing the phase of the oscillations. Then, the process repeats again and again. So, the transformation of the phase at each next cycle of the excitation exchange corresponds to expanding circle map, or Bernoulli map, $\varphi_{n+1} = 2\varphi_n + \text{const}$. As known, this map gives rise to chaotic dynamics with positive Lyapunov exponent $\Lambda = \ln 2 > 0$.

These considerations suggest that at $\mu = \mu_c$ a variant of blue sky bifurcation occurs, which corresponds to the case m=2. So, in accordance with argumentation of Shilnikov and Turaev, it should be accompanied by a birth of hyperbolic attractor, the Smale–Williams solenoid in the Poincaré section.

Figure 2 shows portraits of phase trajectories in projection on the plane of real amplitudes of two oscillators as obtained from numerical solution of Eqs. (2) by the Runge–Kutta method. Parameter values in the computations are $\omega_0 = 2\pi$ and $\varepsilon = 0.5$.

Taking into account configuration of the attractor, in the supercritical domain $\mu > \mu_c$ it is appropriate to define the Poincaré section with a hypersurface S in the for-dimensional phase space by equation $|a_2| = c$ taking into account only crossings in direction of increase of $|a_2|$ (see a horizontal segment and an arrow in panel (b) of Fig. 2). In the parameter range of interest, an appropriate value of the constant is c=2.5. The Poincaré map was realized as a computer program basing on numerical solution of differential equations (2) complemented with procedure of Hénon [18], consistent in accuracy with the applied finite-difference scheme.

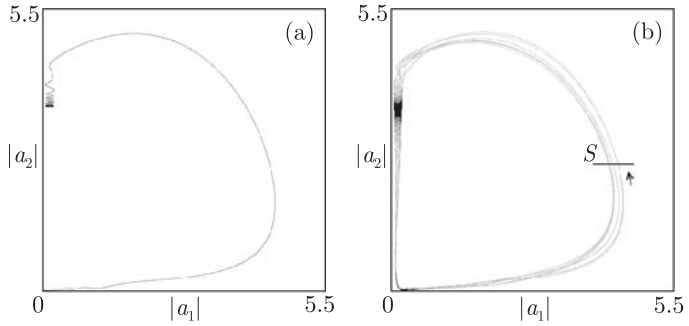

Fig. 2. A transient trajectory (gray) and the limit cycle (black) before the bifurcation at μ=3.14 (a), and portrait of chaotic attractor after the bifurcation, at μ=3.1442 (b), projected onto a plane of real amplitudes $|a_1|$ and $|a_2|$. Other parameters are $\omega_0 = 2\pi$ and $\varepsilon = 0.5$.

As mentioned in [13], near the bifurcation, the characteristic time of return of orbits at the Poincaré section depends on the control parameter like $T(\mu) \sim 1/\sqrt{\mu - \mu_c}$. In computations, the numerical data are found to be in good agreement with this relation. The evidence is delivered by a plot of squared inverse averaged return time against parameter μ (Fig. 3). The bifurcation threshold corresponds to intersection of the curve with the horizontal coordinate axis, and locally the dependence is linear (see the dotted line). From extrapolation, the bifurcation is located with high accuracy at $\mu_c \approx 3.144196$.

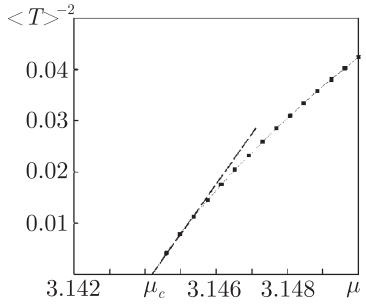

Fig. 3. Squared inverse averaged time of returns at the Poincaré section for orbits on the attractor versus control parameter μ. The blue sky bifurcation point corresponds to μ_c.

Diagrams in Fig. 4 illustrate evolution of phases at successive crossings of the Poincaré section S in the course of motion on the attractor. The phase Φ_n relates to the first oscillator at $t = t_n$, which is the n-th crossing of the orbit with the hypersurface S in the correct direction. In computations, it is determined as $\Phi_n = \arg a_1(t_n)$. Observe that topologically the discrete-step evolution of phases corresponds to Bernoulli map: one full revolution for pre-image Φ_n gives rise to two revolutions for the image Φ_{n+1}. Such topological nature of the mapping persists in a wide parameter range above the bifurcation threshold. It supports the qualitative argument that the case m=2 occurs here, associated with presence of Smale–Williams solenoid in the Poincaré map. Fig. 5 shows the attractor portrait in the Poincaré section in projection on the phase plane of the first oscillator. Although it looks like a simple closed curve, a high enough zoom resolves intrinsic transversal Cantor-like structure, which is essential attribute of the Smale–Williams solenoid.

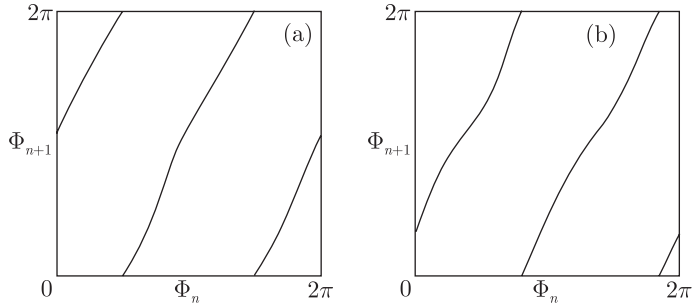

Fig. 4. Diagrams for discrete-step evolution of phases for the first oscillator at passages of the Poincaré section S. Parameters are $\omega_0 = 2\pi$, $\varepsilon = 0.5$, $\mu = 3.1442$ (a) and $\mu = 3.15$ (b).

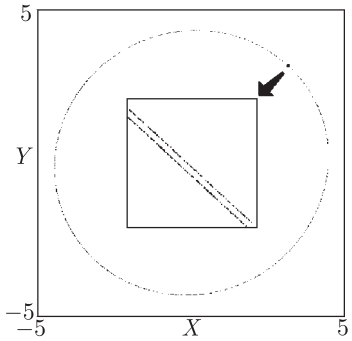

Fig. 5. Attractor of the system (2) at μ=3.15 in the Poincaré section projected onto the phase plane of the first oscillator. Transversal Cantor-like structure becomes visible at great resolution, as shown in the inset.

For computation of Lyapunov exponents, standard algorithm of Benettin [19] was used. Numerical solution of Eqs. (2) on a sufficiently long time interval is performed for the dynamics on

the attractor, together with collection of linearized equations for four perturbation vectors. After some appropriately chosen time period, Gram – Schmidt process is applied to the vectors with their subsequent normalization (reduction to the unit norms). Lyapunov exponents are obtained from slopes of the straight lines approximating the accumulating sums of logarithms of the norms of the vectors (after orthogonalization but before normalization), in dependence on a number of steps of the algorithm.

In Fig. 6 a plot for the Lyapunov exponents is shown, as they behave under parameter variation through the blue sky catastrophe, which occurs at $\mu = \mu_c$ (see panel (a)). In the left part of the plot, the largest Lyapunov exponent is zero, and three others are negative. Here attractor is a stable limit cycle, like that in Fig. 2a. At the bifurcation, both two larger exponents meet at zero, and two others remain negative. After the bifurcation, there is one positive exponent, which grows with increase of μ. The second exponent remains zero, and two others are negative, with gradually decreasing absolute value. Here the Smale–Williams attractor persist. In particular, at μ=3.15 the Lyapunov exponents are

$$\lambda_1 = 0.0434,\ \ \lambda_2 = 0.0000,\ \ \lambda_3 = -8.75,\ \ \lambda_4 = -8.85.$$

The second exponent is zero (up to numerical error) and must be regarded as associated with neutral infinitesimal perturbation along the trajectory on the attractor. Estimate of the attractor dimension from the Kaplan–Yorke formula [20] yields $D_L = 2 + \lambda_1/|\lambda_3| \approx 2.005$.

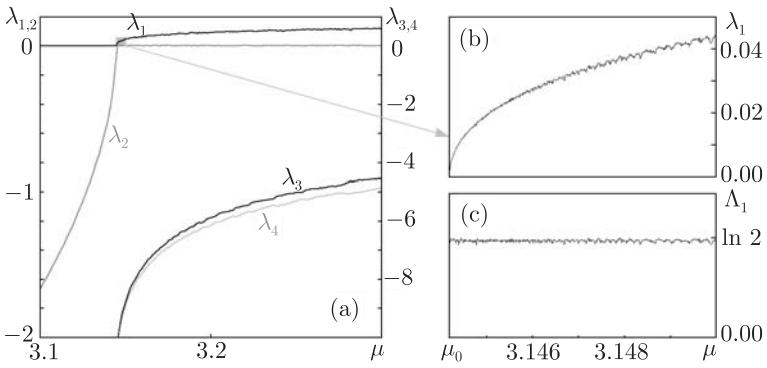

Fig. 6. Lyapunov exponents of the system (2) plotted versus parameter μ (a), a magnified part for the largest Lyapunov exponent near the bifurcation threshold in supercritical domain (b), and the plot for the Lyapunov exponent of the Poincaré map (c). Observe that the Lyapunov exponent for the Poincaré map is approximately constant close to ln 2 that corresponds to the Bernoulli map.

The growth of the positive Lyapunov exponent in the supercritical domain, $\mu > \mu_c$ (see a separate plot (b)) occurs because of decrease of the characteristic time scale observed with growth of distance from the bifurcation point. In the supercritical domain, one can determine Lyapunov exponents Λ_1, Λ_2, Λ_3 for the Poincaré map as well. The zero-value exponent is excluded, and others are in obvious relation with those for the differential equations, namely, $\Lambda_1 = \lambda_1 < T >$, $\Lambda_2 = \lambda_3 < T >$, $\Lambda_3 = \lambda_4 < T >$. Here $< T >$ is characteristic time of return at the Poincaré section, averaged over orbits on the attractor. Observe that the positive exponent for the Poincaré map remains almost constant in a wide parameter range (up to fluctuations because of the numerical inaccuracy). It is close to $\ln 2$, the value corresponding to the Bernoulli map (see panel (c) in Fig. 6).

In conclusion, this article presents an explicit four-dimensional dissipative system manifesting a variant of blue sky catastrophe accompanied with birth of attractor of Smale–Williams type in the return map. All features of the transition observed in the computations agree well with the theory developed by Shilnikov and Turaev.

The model essentially supplements a collection of known examples of blue sky catastrophes [14–16] restricted until now with transitions involving only regular attractors, the limit cycles. This and similar model systems may be of interest for understanding variety of dynamical behaviors, e.g. in neurodynamics: Indeed, some models with the blue sky catastrophes relate to this discipline [15, 16], as well as a hypothetical example of a uniformly hyperbolic strange attractor suggested in [21].

The research is supported, in part, by RFBR-DFG grant 08-02-91963 and by grant 2.1.1/1738 of Ministry of Education and Science of Russian Federation in a frame of program of Development of Scientific Potential of Higher Education. The author thanks A. Pikovsky and I. Sataev for discussions.

REFERENCES

1. Eckmann, J.-P. and Ruelle, D., Ergodic Theory of Chaos and Strange Attractors, *Rev. Mod. Phys.*, 1985, vol. 57, pp. 617–656.
2. Shil'nikov, L., Mathematical Problems of Nonlinear Dynamics: A Tutorial, *Int. J. of Bifurcation and Chaos*, 1997, vol. 7, pp. 1353–2001.
3. Katok, A. and Hasselblatt, B., *Introduction to the Modern Theory of Dynamical Systems,* Cambridge: Cambridge University Press, 1996.
4. Hasselblatt, B. and Katok, A., *A First Course in Dynamics: with a Panorama of Recent Developments*, Cambridge: Cambridge University Press, 2003.
5. Afraimovich, V. and Hsu, S.-B., *Lectures on Chaotic Dynamical Systems*, AMS/IP Studies in Advanced Mathematics, vol. 28, Providence, RI: Amer. Math. Soc., Somerville, MA: International Press, 2003.
6. Plykin, R.V., Sources and Sinks of A-diffeomorphisms of Surfaces, *Math. USSR Sb.*, 1974, vol. 23, no. 2, pp. 233–253.
7. Hunt, T.J. and MacKay, R.S., Anosov Parameter Values for the Triple Linkage and a Physical System with a Uniformly Chaotic Attractor, *Nonlinearity*, 2003, vol. 16, pp. 1499–1510.
8. Kuznetsov, S.P., Example of a Physical System with a Hyperbolic Attractor of the Smale–Williams Type, *Phys. Rev. Lett.*, 2005, vol. 95, 144101.
9. Kuznetsov, S.P. and Seleznev, E.P., Strange Attractor of Smale–Williams Type in the Chaotic Dynamics of a Physical System, *Zh. Eksper. Teoret. Fiz.*, 2006, vol. 129, no. 2, pp. 400–412 [*J. Exp. Theor. Phys.*, 2006, vol. 102, no. 2, pp. 355–364].
10. Ruelle, D. and Takens, F. On the Nature of Turbulence, *Comm. Math. Phys.*, 1971, vol. 20, no. 3, pp. 167–192.
11. Newhouse, S., Ruelle, D., and Takens, F., Occurrence of Strange Axiom A Attractors near Quasiperiodic Flows on T^m, $m \geqslant 3$, *Comm. Math. Phys.*, 1978, vol. 64, no. 1, pp. 35–40.
12. Shil'nikov, L.P. and Turaev, D.V., Blue Sky Catastrophes, *Dokl. Akad. Nauk*, 1995, vol. 342, no. 5, pp. 596–599 (Russian).
13. Shil'nikov, L.P. and Turaev, D.V., Simple bifurcations leading to hyperbolic attractors, *Computers & Mathematics with Applications*, 1997, vol., nos. 2-4, pp. 173-193.
14. Gavrilov, N. and Shilnikov, A., Example of a blue sky catastrophe, *'Methods of qualitative theory of differential equations and related topics, AMS Transl. Series II*, 2000, vol. 200, pp. 99-105.
15. Shilnikov, A. and Cymbalyuk, G., Transition between Tonic Spiking and Bursting in a Neuron Model via the Blue Sky Catastrophe, *Phys. Rev. Lett.,* 2005, vol. 94, no.4, 048101.
16. Shilnikov, A. and Kolomiets, M., Methods of the Qualitative Theory for the Hindmarsh–Rose Model: A Case Study, *Int. J. of Bifurcation and Chaos*, 2008, vol. 18, no. 8, pp. 2141–2168.
17. Kuznetsov, S.P. and Pikovsky, A. Autonomous Coupled Oscillators with Hyperbolic Strange Attractors, *Physica D*, 2007, vol. 232, pp. 87–102.
18. Henon, M., On the Numerical Computation of Poincaré Maps, *Physica D*, 1982, vol. 5, nos 2–3, pp. 412–414.
19. Benettin, G., Galgani, L., Giorgilli, A., and Strelcyn, J.-M., Lyapunov Characteristic Exponents for Smooth Dynamical Systems and for Hamiltonian Systems: A Method for Computing All of Them, *Meccanica*, 1980, vol. 15, pp. 9–30.
20. Kaplan, J.L. and Yorke, J.A., Chaotic Behavior of Multi-dimensional Differential Equations, in: *Functional Differential Equations and Approximations of Fixed Points*, Peitgen, H.O. and Walther, H.O. (Eds.), Lecture Notes in Mathematics, vol. 730, 1979, pp. 204–227.
21. Belykh, V., Belykh, I., and Mosekilde, E., The Hyperbolic Plykin Attractor Can Exist in Neuron Models, *Int. J. of Bifurcation and Chaos*, 2005, vol. 15, no. 11, pp. 3567–3578.